# Design, Fabrication and Comprehensive Testing of Biodegradable 3D Printable Hybrid Polymer Airway Splints

**Sonali S. Naik[1,2,3], Jitraporn Vongsvivut[4], Chaitali Dekiwadia[5], Amanda N. Abraham[6], Naba K. Dutta[3*], Namita Roy Choudhury[3*] and Kiran Sukumaran Nair[1,2*]**

[1] Polymer Science and Engineering, CSIR-National Chemical Laboratory, Pune, India

[2] Academy of Scientific and Innovative Research (AcSIR), Ghaziabad – India

[3] School of Engineering, RMIT University, Melbourne, VIC, 3000, Australia

[4] Infrared Microspectroscopy (IRM) beamline, ANSTO—Australian Synchrotron, 800 Blackburn Road, Clayton, VIC 3168, Australia

[5] RMIT Microscopy and Microanalysis Facility, RMIT University, Melbourne, VIC, Australia

[6] School of Science, RMIT University, Melbourne, VIC 3000, Australia

## Supplementary data

### 1. Reaction conditions for the synthesis of pec-g-PCL

Table S1: The reaction conditions for the copolymerization of pectin and ε-caprolactone (CL), along with the corresponding grafting ratio, pectin weight percentage in the copolymer are as follows

| | Polymer | Ratio | W1(g) (Pectin) | W2(g) (CL) | Temp (°C) | Time (hrs) | Yield (%) | GR (%) |
|---|---|---|---|---|---|---|---|---|
| 1 | P1 | 1:5 | 1 | 5 | 100 | 16 | 74.8 | 16.67 |
| 2 | P2 | 1:10 | 0.5 | 5 | 100 | 16 | 83.6 | 29.24 |
| 3 | P3 | 1:25 | 0.2 | 5 | 100 | 16 | 98.8 | 54.86 |
| 4 | P4 | 1:50 | 0.1 | 5 | 100 | 16 | 99.0 | 78.46 |
| 5 | P5 | 1:100 | 0.05 | 5 | 100 | 16 | 97.4 | 79.62 |

The grafting content of the PCL component in the polymers was assessed using the signal intensities of the CL unit and the pectin unit. The H-2 proton signal from pectin, which appears at 3.46 ppm, is distinctly separated from the a, b, and c-protons of the CL unit that are found in

the range of 1.2 to 1.5 ppm. Therefore, the grafting content of the PCL branches can be calculated accordingly [1].

$$\text{PCL grafting content\%} = \frac{114 \times I(1.2 - 1.5ppm)}{194 \times 6I(3.46ppm)} \quad \text{----------Eq S1}$$

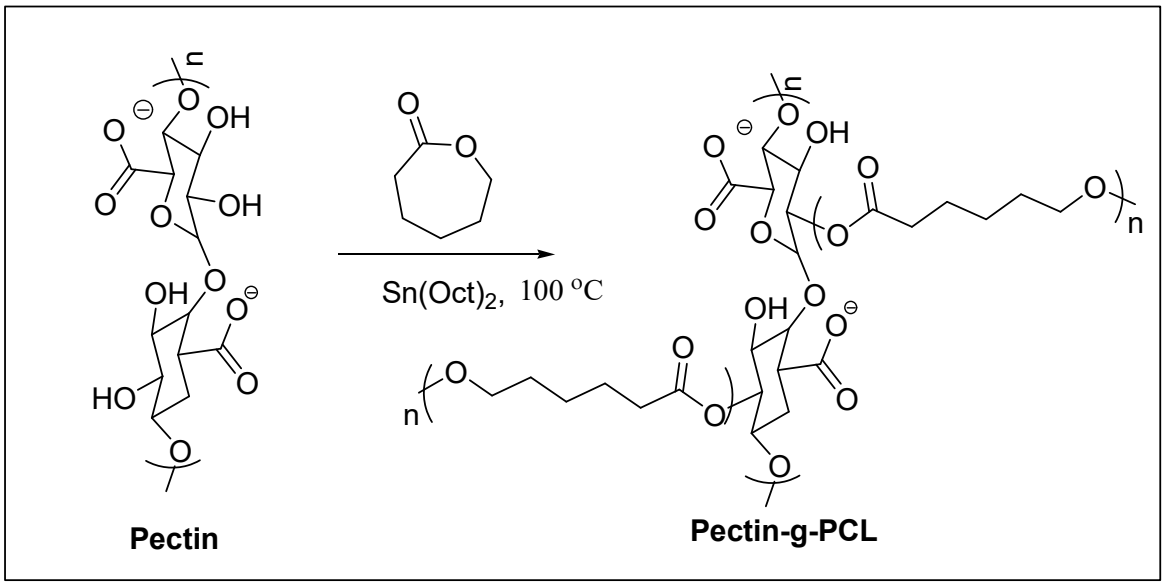


Scheme S1: Synthesis of pec-g-PCL by ring-opening polymerization

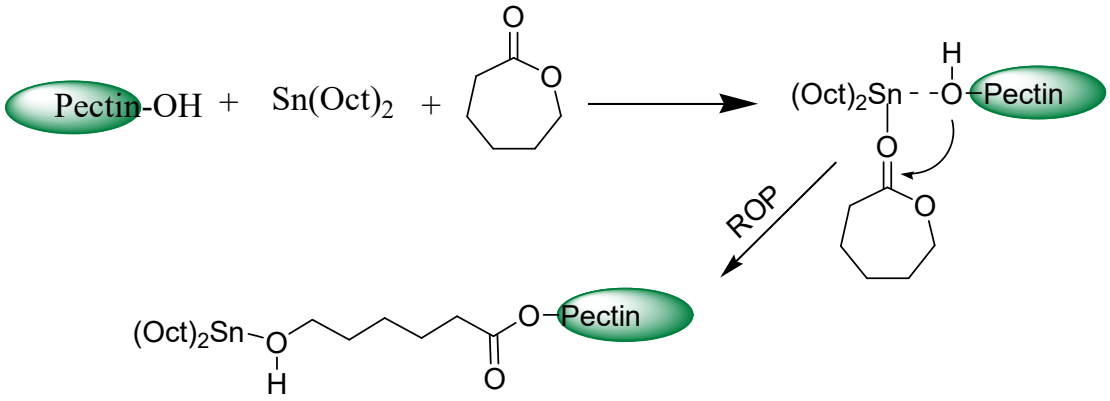


Scheme S2: Grafting mechanism of CL on pectin by ROP

## 2. FTIR spectroscopy of pec-g-PCL polymers

The distinctive peak at 3200 $cm^{-1}$ to 3650 $cm^{-1}$ in pectin and PCL corresponds to secondary alcohol OH stretching. Symmetric and asymmetric C-H stretching was observed at 2954 $cm^{-1}$, and characteristic C=O peaks were detected in the range of 1750-1700 $cm^{-1}$. The typical peak in the 1170-1150 $cm^{-1}$ range is related to C-O-C stretching vibration. The C=O stretching of both PCL and pectin overlaps in the 1750-1700 $cm^{-1}$ range, forming a high-intensity peak.

## 3. Boundary conditions and parameters used for FEA

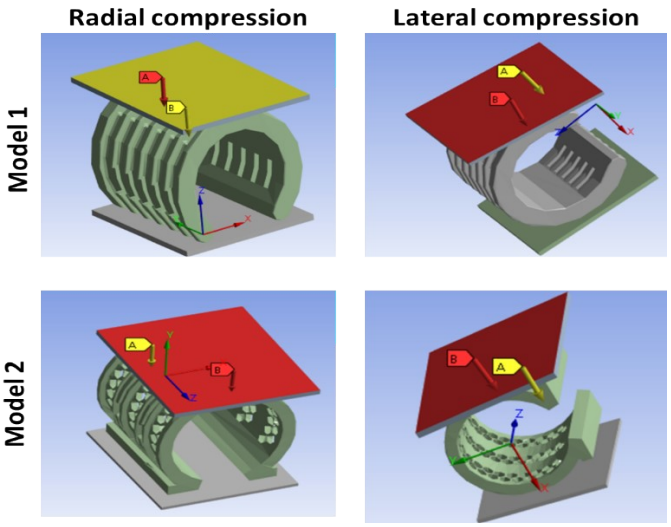


Figure S1: Boundary conditions for the FEA test

Table S2: Parameters used for FEA

| Property | Value | Unit |
|---|---|---|
| Density | 1145 | Kg/m3 |
| **Isotropic elasticity** | | |
| Youngs modulus | 200 | MPa |
| Poissons ratio | 0.3 | |
| Bulk modulus | 1.6667E+08 | Pa |
| Shear modulus | 7.6923E+07 | Pa |
| Force | 500 | N |
| Thermal conductivity | 0.05 | W/mK |

## 4. $^{1}$H NMR spectroscopy of pec-g-PCL polymers

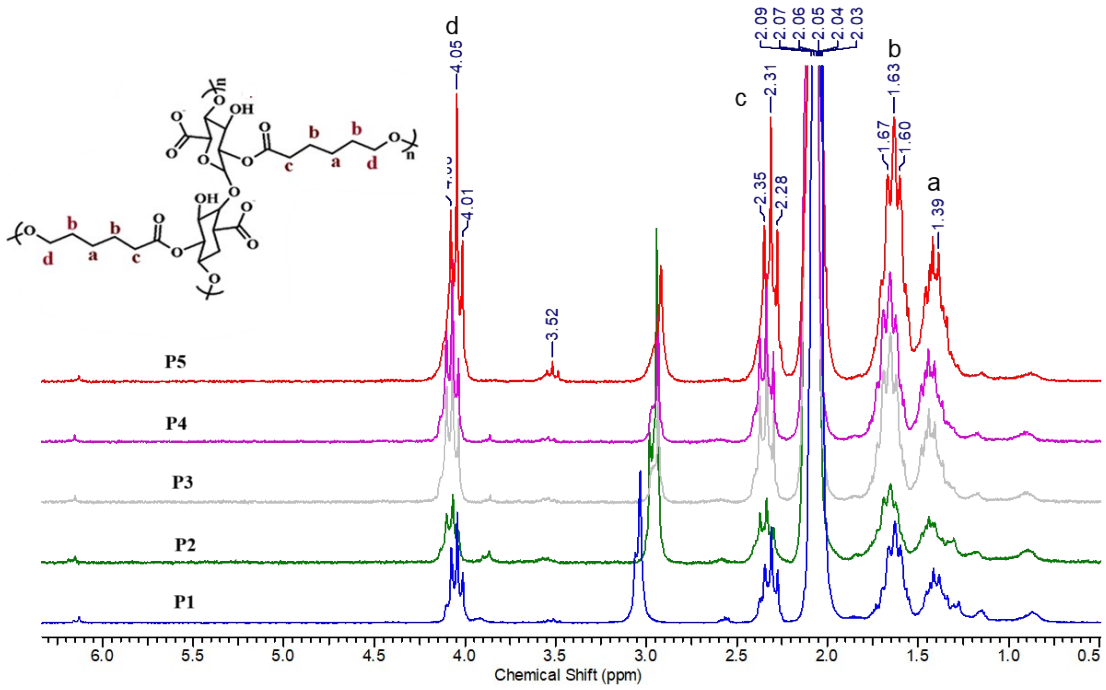


Figure S2: [1]H NMR spectra of different compositions of pec-g-PCL

## 5. Thermal and XRD analysis of pec-g-PCL polymers

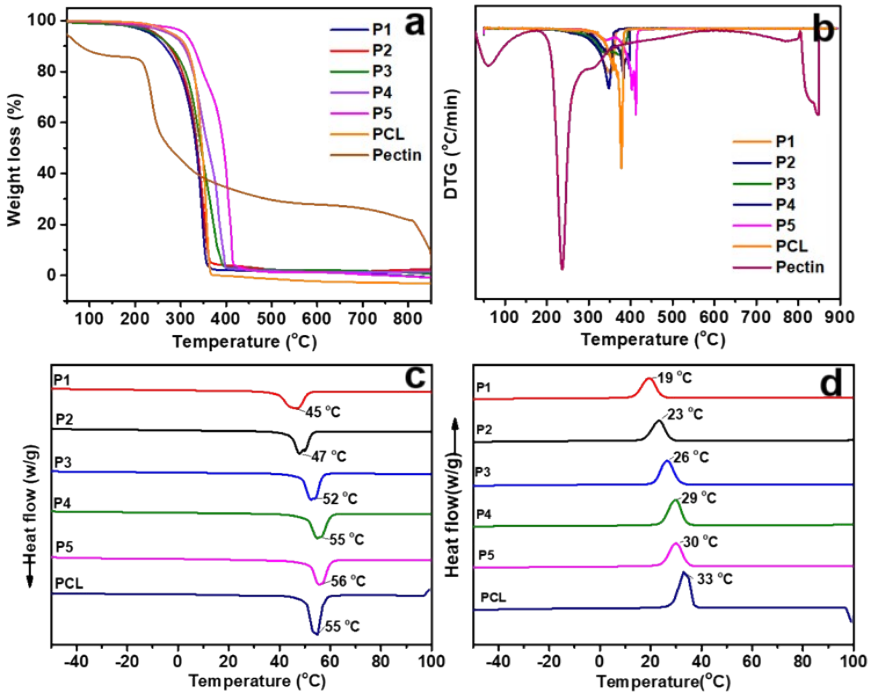


Figure S3: a) TGA curves of Pectin and pec-g-PCL b) DTGA curves of pectin and pec-g-PCL c) DSC melting endotherm of pec-g-PCL polymers d) DSC cooling exotherm of pec-g-PCL

Table S3: Crystallization properties of pec-g-PCL polymers

| Sl.no | | P1 | P2 | P3 | P4 | P5 | PCL |
|---|---|---|---|---|---|---|---|
| 1 | L (110) nm | 25.21 | 17.42 | 23.14 | 26.18 | 28.39 | 19.71 |
| 2 | L (111) nm | 19.5 | 13.61 | 19.09 | 23.39 | 23.63 | 11.56 |
| 3 | $X_{c\ DSC}$ | 20.89 | 27.33 | 30.123 | 34.80 | 36.01 | 49 |
| 4 | $X_{c\ XRD}$ | 29.80 | 31.93 | 32.88 | 33.13 | 31.73 | 57 |

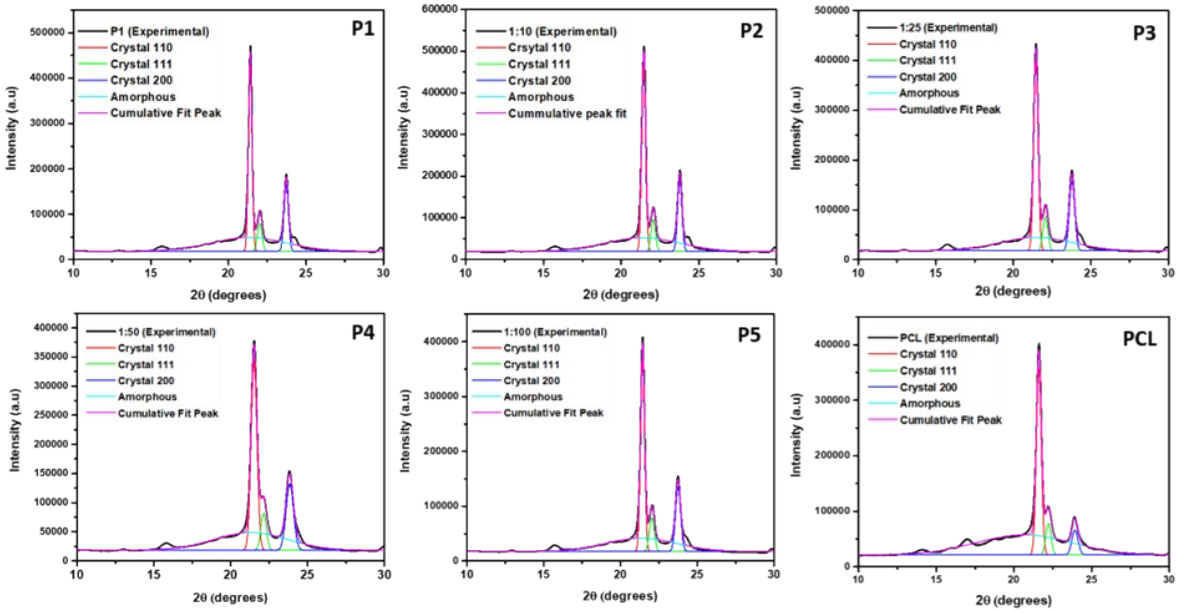


Figure S4: Fitting of scattering profile from XRD analysis of pec-g-PCL polymers (P1 to P5)

## 6. Rheological study of pec-g-PCL polymers

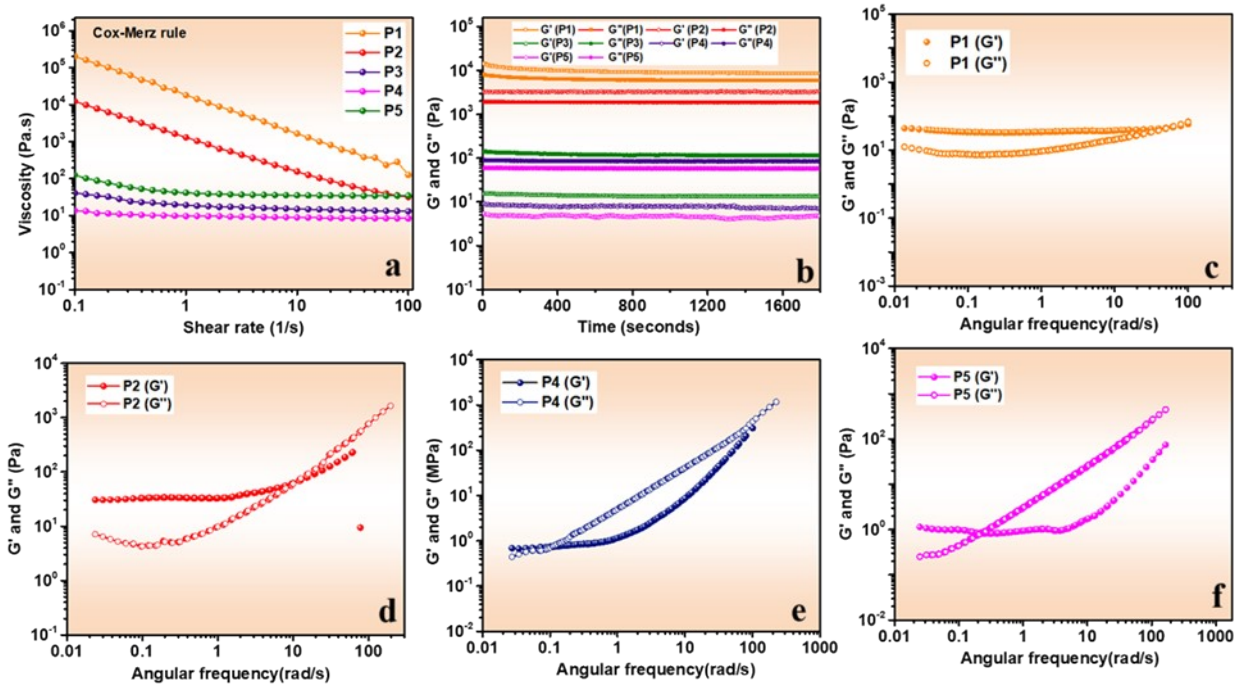


Figure S6: Rheological study of pec-g-PCL polymers a) Cox-merz rule b) Time sweep experiment of pec-g-PCL polymers @frequency 10rad/s strain % temperature: 70°C; c-f) TTS analysis of pec-g-PCL polymers

Table S4: Printing parameters for 3D printing Pec-g-PCL

| **Pectin-g-PCL** | **Temp(°C)** | **Pressure(PSI)** | **Printing speed(mm/s)** | **Layer height (mm)** | **Printing accuracy (%)[a]** |
|---|---|---|---|---|---|
| P1 | 70 | 2 | 2 | 0.1 | - |
| P2 | 70 | 2 | 2 | 0.1 | 66.66 |
| P3 | 70 | 3 | 2 | 0.1 | 80 |
| P4 | 70 | 5 | 2 | 0.1 | 77.4 |
| P5 | 70 | 8 | 2 | 0.1 | 70.95 |

[a]$P = (1-\frac{Wi-W}{W})\times 100$, Printed width is calculated using Image J software considering a minimum of 6 measurements.

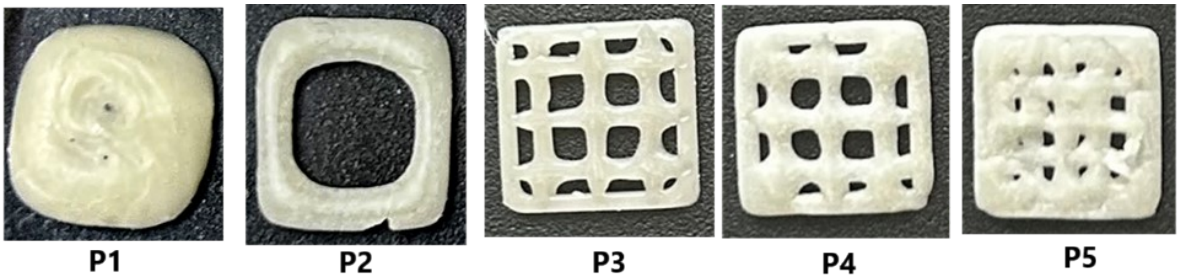

Figure S7: 3D printability test of Pec-g-PCL polymers

## 7. Micro-CT analysis of tracheal splints

Table S5: Micro-CT data of 3D printed tracheal splints

| Tracheal models | Porosity µ-CT (%) | Porosity CAD (%) | Solid volume CAD ($mm^3$) | Total volume CAD ($mm^3$) | Closed pore volume ($mm^3$) | Closed porosity (%) | Open porosity (%) | Printing resolution (%) |
|---|---|---|---|---|---|---|---|---|
| PCL-M1 | 65.5 | 77.3 | 227 | 1000 | 0.68 | 0.648 | 64.9 | 99±2 |
| PCL-M2 | 80.6 | 83.3 | 289 | 1727 | 0.5 | 0.322 | 80.3 | 98±3 |
| P3-M1 | 73.5 | 77.3 | 227 | 1000 | 0.375 | 0.162 | 73.3 | 80±0.4 |
| P3-M2 | 81.6 | 83.3 | 289 | 1727 | 0.686 | 0.134 | 81.4 | 82±0.5 |

The porosity of the CAD models was obtained by measuring the occupied volume of each scaffold, and the designed porosity ($P_{CAD}$) was calculated as follows Equation (S2):

$$P_{CAD} = 1 - {}^{Vf}/_{Vt} * 100 \text{----------Eq S2}$$

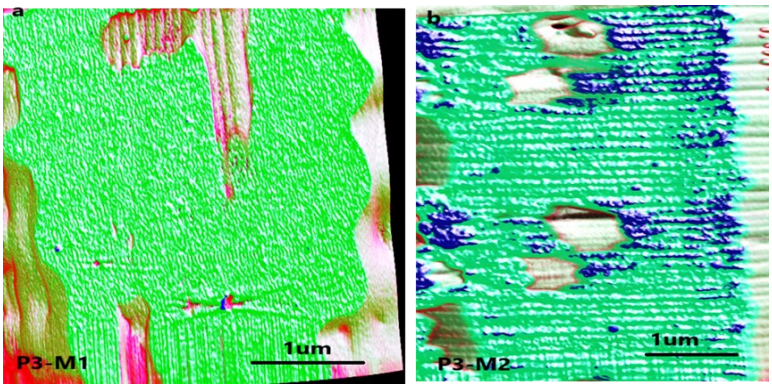

**Figure S8**: Voids observed on the 3D printed pec-g-PCL splints

## 8. Mechanical testing of 3D-printed splints

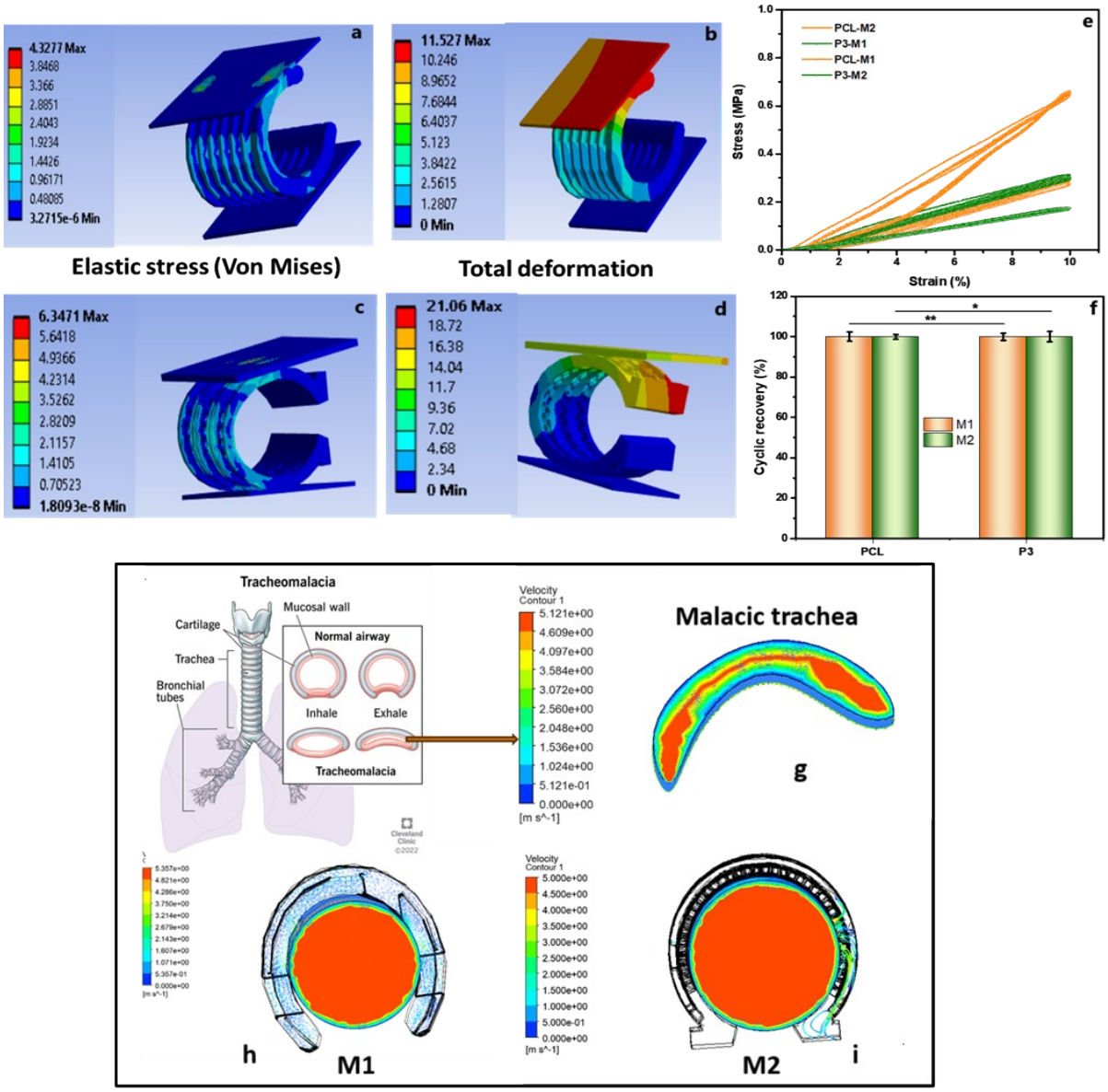


**Figure S9**: a-d) FEA analysis of splints under lateral compression e) Cyclic testing under lateral compression f) Cyclic recovery of 3D printed splints g) Air flow through diseased trachea h, i) outlet velocity of air through the tracheal lumen after splint placement

## 9. Degradation studies

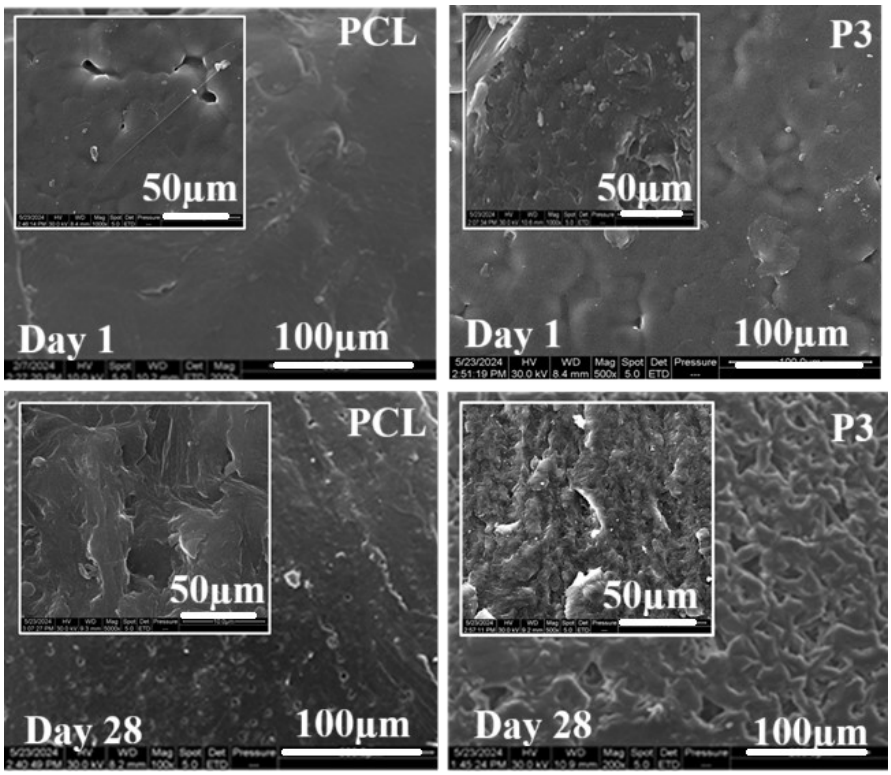


**Figure S10**: Degradation Studies. (a) SEM images showing the morphology of degraded samples under accelerated conditions.

## 10. Cell culture studies

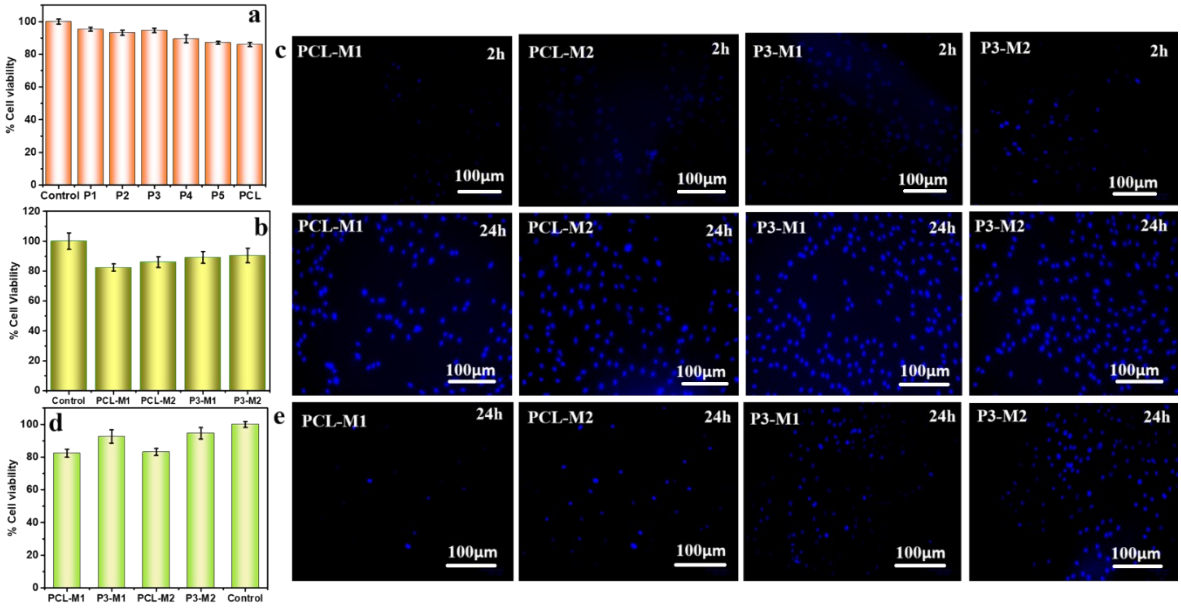

**Figure S11**: a) Cell viability of L929 cells on pec-g-PCL polymers b) Cell viability of L929 cells on 3D printed splints c) DAPI staining of cells attached on 3D printed splints after 2 hours and 24 hours of incubation d) Cell viability of hMSC cells on 3D printed splints e) DAPI staining of hMSC cells attached on 3D printed splints after 24 hours of incubation

**References**

(1) Liu, L.; Li, Y.; Liu, H.; Fang, Y. Synthesis and Characterization of Chitosan-Graft-Polycaprolactone Copolymers. *Eur Polym J* **2004**, *40* (12), 2739–2744. https://doi.org/10.1016/j.eurpolymj.2004.07.016.